Fast-ion D_α spectrum diagnostic in the EAST

Y. M. Hou,[1,2] C. R. Wu,[1] J. Huang,[1,a)] W. W. Heidbrink,[3] M. G. von Hellermann,[4] Z. Xu,[1] Z. Jin,[1] J. F. Chang,[1] Y. B. Zhu,[3] W. Gao,[1] Y. J. Chen,[1] B. Lyu,[1] R. J. Hu,[2] P. F. Zhang,[1] L. Zhang,[1] W. Gao,[1] Z. W. Wu,[1] Y. Yu,[2] M. Y. Ye,[2] and EAST Team[1,b)]

[1]*Institute of Plasma Physics, Chinese Academy of Sciences, P.O. Box 1126, Hefei, Anhui 230031, China*
[2]*School of Nuclear Science and Technology, University of Science and Technology of China, Hefei, Anhui 230026, China*
[3]*Department of Physics and Astronomy, University of California, Irvine, California 92697, USA*
[4]*Diagnostic Team, ITER Organization, Route de Vinon-sur-Verdon, Saint Paul Lez Durance 13067, France*

(Presented 8 June 2016; received 6 June 2016; accepted 13 July 2016; published online 26 September 2016)

In toroidal magnetic fusion devices, fast-ion D-alpha diagnostic (FIDA) is a powerful method to study the fast-ion feature. The fast-ion characteristics can be inferred from the Doppler shifted spectrum of D_α light according to charge exchange recombination process between fast ions and probe beam. Since conceptual design presented in the last HTPD conference, significant progress has been made to apply FIDA systems on the Experimental Advanced Superconducting Tokamak (EAST). Both co-current and counter-current neutral beam injectors are available, and each can deliver 2-4 MW beam power with 50-80 keV beam energy. Presently, two sets of high throughput spectrometer systems have been installed on EAST, allowing to capture passing and trapped fast-ion characteristics simultaneously, using Kaiser HoloSpec transmission grating spectrometer and Bunkoukeiki FLP-200 volume phase holographic spectrometer coupled with Princeton Instruments ProEM 1024B eXcelon and Andor DU-888 iXon3 1024 CCD camera, respectively. This paper will present the details of the hardware descriptions and experimental spectrum. *Published by AIP Publishing.* [http://dx.doi.org/10.1063/1.4960598]

I. INTRODUCTION

Fast ions in toroidal magnetic fusion devices are produced by fusion reactions, neutral beam injection (NBI), and ion cyclotron acceleration. They can also be a major source of plasma heating and current drive. Therefore, the investigation of the characteristics of the fast-ion transport is important to understand plasma confinement. The fast-ion characteristics can be inferred from the Doppler shifted spectrum of D_α light according to charge exchange recombination process between fast ions and probe beam. Since fast-ion D-alpha diagnostic (FIDA)[1] was first commissioned on DIII-D[2] in 2004, it has been applied by many devices for its powerful capability, such as NSTX,[3] TEXTOR,[4] LHD,[5] ASDEX-U,[6] MAST,[7] and experimental advanced superconducting tokamak (EAST).[8]

EAST is a fully superconducting tokamak experimental device, with the major radius of 1.85 m and the minor radius of 0.5 m. Auxiliary heating systems on EAST have been improved and upgraded: both co-current and counter-current neutral beam injectors (NBIs) are available, and each can deliver 2-4 MW beam power with 50-80 keV beam energy; the lower hybrid current drive (LHCD) systems have been upgraded to 2.45 GHz/4 MW and 4.6 GHz/6 MW; and the total power of ion-cyclotron resonance heating (ICRH) systems can be up to 12 MW. These can produce a non-Maxwellian anisotropic high energetic ion population, which can contribute to plasma heating and current drive, and also can cause damage to the first wall. Several other new complementing techniques are also under development to study the fast-ion behavior, e.g., neutral particle analyzers (NPAs),[9] fast-ion loss detectors (FILDs), gamma camera, and neutron camera.

Since conceptual design presented in the last HTPD conference,[8] significant progress has been made to improve the capability and stability of FIDA systems on EAST. The s-FIDA and f-FIDA constitute FIDA system. The s-FIDA obtains D_α spectrum with two spectrometers, while the f-FIDA obtains wavelength-integrated signals with a band-pass filter and a multianode photomultiplier tube (PMT). This paper will present the details of the hardware descriptions and experimental spectrum of s-FIDA.

This article is structured as follows: Section II shows the diagnostic layout on EAST. Details of instrumental performance are described in Section III. Section IV presents recent experimental data from the 2016 EAST campaign.

II. DIAGNOSTIC LAYOUT

Fig. 1 shows the general layout: (a) plan view of EAST with two available injectors on A-port and F-port, including two beam sources of each. The tangential and vertical views are corresponding to the O horizontal and B vertical port, covering the region of major radii from 177 cm to 237 cm, and from 177 cm to 205 cm, respectively. There are two common measures for background subtraction: beam modulation and the paired active and passive view method. The passive N-port

Note: Contributed paper, published as part of the Proceedings of the 21st Topical Conference on High-Temperature Plasma Diagnostics, Madison, Wisconsin, USA, June 2016.

a)Electronic mail: juan.huang@ipp.ac.cn

b)See Appendix of B. N. Wan *et al.,* Nucl. Fusion **55**, 104015 (2015).

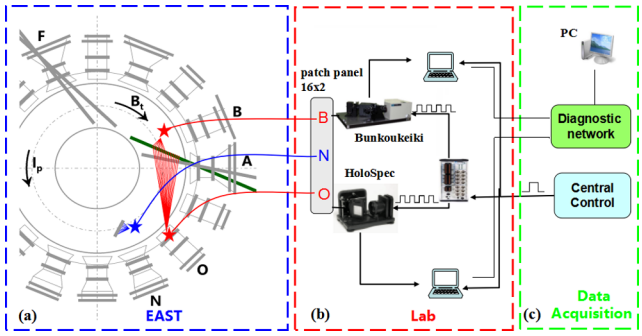

FIG. 1. (a) Plan view of EAST showing tangential views and vertical views on O-port and B-port, respectively. The passive N-port views are geometrically same as active B-port views. (b) The s-FIDA instruments in laboratory and (c) data acquisition systems.

views are geometrically same as active B-port views. So they are designed for background subtraction. For the tangential view, it was used to observe the beam from behind. Due to the limitation of the viewing port, a reflector, which is coated with 900 Å aluminium for high reflectance, is applied to traverse the lights.[10] After the reflection, the lights are collected by a series of lens. The lens focuses 16 channels onto a fiber optic array each with 1500 μm core diameter, corresponding to the radial spot size at the mid-plane around 3 cm. Matching the fiber optics numerical aperture of 0.37, the lens has the diameter of 87 mm, the focal length of 114.5 mm with high transparency (≥99.6%) at 650.0 nm. For the vertical view, a series of lens, with the diameter of 40.4 mm, the focal length of 55.2 mm, are located at the B-port and the N-port. They collect and focus light onto an 8-channel fiber optic array. With length about 50 m, the optical fibers guide the signals to the s-FIDA instruments in the FIDA diagnostic room, shown in Fig. 1(b), keeping the detectors away from neutrons and gamma emission. Patch panels for the optical fiber link from observation ports to the instruments allow a flexible combination of ports and instruments. To obtain good spectral resolution and temporal resolution, high resolution spectrometers are applied. The detailed specifications will be discussed in Section III.

The requirements of the timing triggers for FIDA diagnostics are shown in Fig. 1(c). The trigger device is applied to trigger the spectrometers with exact timing sequence and synchronize exposure time. The PCI-6602 timing card of National Instruments is inserted into the personal computer (PC) and configured to generate various trigger pulses. This type of timing card has one input trigger channel and seven output trigger channels. The exposure time, acquiring rate (smaller than the readout rate, or some frames will be lost), and delay time should be modified according to the parameters of each shot. Shot number and default pulse length of each shot are sent out by main control system and received by each diagnostic. After the preparation of 60 s, a trigger signal is re-sent and all diagnostic systems start to work. Meanwhile, a series of trigger pulses are generated by the trigger device and used to set the exposure time of each CCD. The cameras use the frame-transfer mode. Kaiser has 16 binning channels and readout time is 7.15 ms. LightField software distributed by Princeton Instruments is configured to acquire data. Bunkoukeiki has 16 binning channels too, while the read out time is 6.08 ms. Andor SOLIS software distributed by Andor is applied to obtain signals. The Central Control sends out a network signal with shot number and start pulse to all systems. Thus the slave PCs of trigger device and spectrometers start running program and setting acquiring frames when they get the network signal, then waiting for the start pulse to generate trigger pulses and acquire data.

III. INSTRUMENT PERFORMANCE

Two spectroscopy systems are currently available: one is HoloSpec transmission grating spectrometer from Kaiser Optical System, with F-number of 1.8, the focal length of 85 mm and the reciprocal linear dispersion of 1.4 nm/mm, coupled with ProEM 1024B eXcelon CCD camera from Princeton Instruments (1024 × 1024 pixels, 13 × 13 μm/pixel). The other is FLP-200 VPH (Volume Phase Holographic) spectrograph system from Bunkoukeiki system, with F-number of 2, the focal length of 200 mm and the reciprocal linear dispersion of 1.28 nm/mm, coupled with DU-888 iXon3 from Andor Instruments (1024 × 1024 pixels, 13 × 13 μm/pixel).

Configuration of Bunkoukeiki FLP-200 VPH spectroscopic system is illustrated in Fig. 2(a). The spectral range of Bunkoukeiki is 643.0–675.5 nm. Referring to the picture, 16 fibers are arranged vertically and fixed well by the fiber holder. The range of adjustment of the entrance slit is 4 mm with 0.01 mm as its minimum step; the grooves number of VPH grating is 2400 g/mm, and its center wavelength is 655.0 nm and incidence/exit angle is 1.8°; the OD3 neutral density filter (see Fig. 2(b)) is mainly used to attenuate brightness interfering signal of D_α at 656.28 nm and LiI at 670.78 nm. The character of the spectrometer (see Fig. 4) determines the shape of the two strips. Optical tests were carried out to ascertain the location of each strip. Besides, each arc strip has a width of 1.5 mm and wavelength width of 1.9 nm.

Kaiser HoloSpec spectroscopic system is illustrated in Fig. 3. The spectral range of Kaiser is from 643.0 nm to 662.0 nm. The breadth of its entrance slit is fixed at 50 μm, and the ratio of output focal length to input focal length is 75/75. Furthermore, its center wavelength of high dispersion VPH grating is 652.5 nm and the OD3 neutral density filter is only at 656.1 nm.

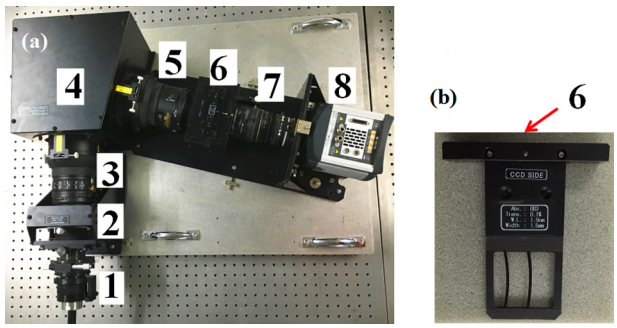

FIG. 2. (a) Configuration of Bunkoukeiki FLP-200 VPH spectroscopic system: (1) the fiber holder; (2) the adjustable entrance slit; (3) the entrance camera lens; (4) the VPH grating; (5) the output lens; (6) the OD3 neutral density filter; (7) the demagnification lens; (8) Andor DU-888 iXon3 1024 CCD camera. (b) Details of the OD3 neutral density filter.

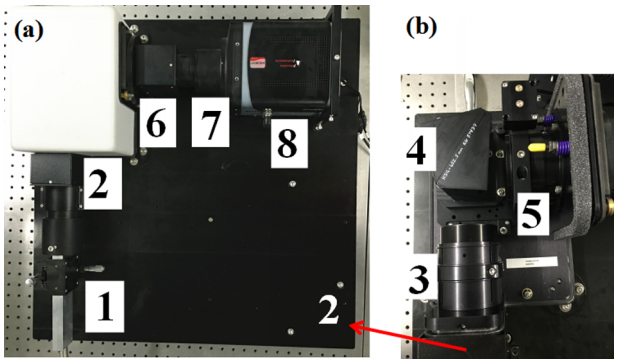

FIG. 3. (a) Picture of Kaiser HoloSpec spectroscopic system; (b) interior of the Kaiser HoloSpec spectrometer. (1) The fiber holder; (2) the fixed entrance slit; (3) the entrance camera lens; (4) the VPH grating; (5) the output lens; (6) the OD3 neutral density filter; (7) the demagnification lens; (8) Princeton Instruments ProEM 1024B eXcelon CCD camera.

The wavelength calibration of each spectrometer was performed with a neon lamp. At the plane of CCD, the light is dispersed into a two dimensional pattern: vertically, separated into 16 chords; horizontally, dispersed in wavelength. As rays from 16 fibers along the vertical slit are incident on the plane grating with different angles, every channel has its own central wavelength result in a parabolic image for Bunkoukeiki and Kaiser measurements.[11,12] Those fitted parabolic lines (see Fig. 4) represent the peaks of a image capture of CCD when every chord is lighted by a neon lamp. And those gray parallel bars show different 16 binning channels on CCD mid-plane. For intensity calibration, tungsten ribbon lamps are normally used for *in situ* absolute calibration and further corrected by the corresponding visible bremsstrahlung measurements.[8] Before applying the calibration factors to the raw data from the CCD, the important step is to correct the raw data with the smear effect[12] that originated from the readout procedure of the CCD. The absolute calibration is accomplished for the data during 2016 spring campaign.

The instrument broadening is obtained by cold line radiation from the neon lamp. Fig. 5(a) shows a comparison of instrument broadening of two spectrometers when the entrance slit is 50 μm.

The different channels of Bunkoukeiki show wider broadening towards the CCD edge up to 0.21 nm and the lowest

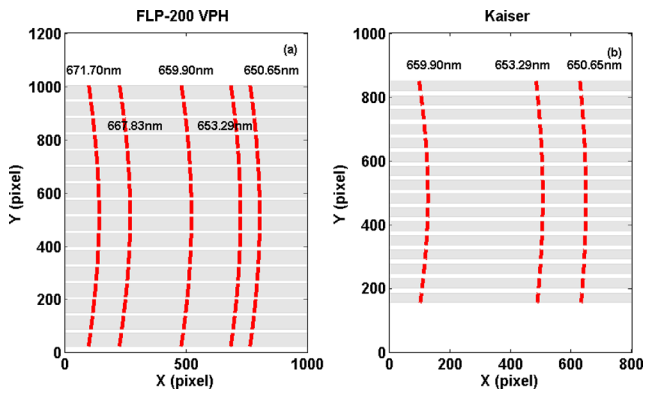

FIG. 4. Picture of fitted parabola of (a) Bunkoukeiki FLP-200 VPH and (b) Kaiser. The gray parallel bars show different 16 binning channels on CCD mid-plane.

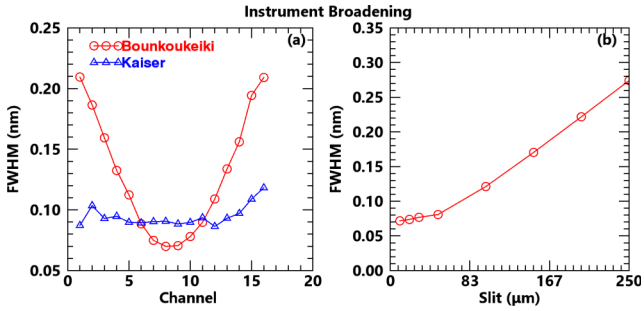

FIG. 5. (a) A comparison of instrument broadening of two spectrometers when the slit is 50 μm; (b) the instrument function of Bunkoukeiki system.

on the center region about 0.06 nm. For Kaiser system, the instrumental function shows near constant for different channel around 0.1 nm. Fig. 5(b) shows the instrument function of Bunkoukeiki system, as the function of the slit width, that the instrument broadening increases with slit width growing.

IV. EXPERIMENTAL DATA

Fig. 6 shows the typical raw spectrum data from vertical and tangential geometry during beam on and beam off period, for only probe beam modulation shots #61821. EAST plasma data: B_t = 2.5 T, $n_e = 3.0 \times 10^{19}$ m^3, T_i = 1.1 keV, and neutral beam energy is 56 keV. The vertical views pick out trapped fast-ions due to their large v_perpendicular, while tangential views pick out passing ions due to their large v_parallel. The spectra consist of impurity line emissions, reduced cold D_α and LiI line emission, and D_α active radiation. The spectrum from vertical view at R = 197 cm, shown in Fig. 6(a), is obtained by Bunkoukeiki system. When the slit width is 200 μm, the instrument broadening is about 0.24 nm. It shows active impurity contribution Ar XVI line at 661.2 nm. Passive non-charge exchange lines as OV line at 650.1 nm, two CII lines at 657.8 nm and 658.3 nm, OII line at 664.1 nm, SiII line at 667.2 nm, and HeI line at 667.9 nm, which appear whether the beam is on or not. There are few impurity line emissions

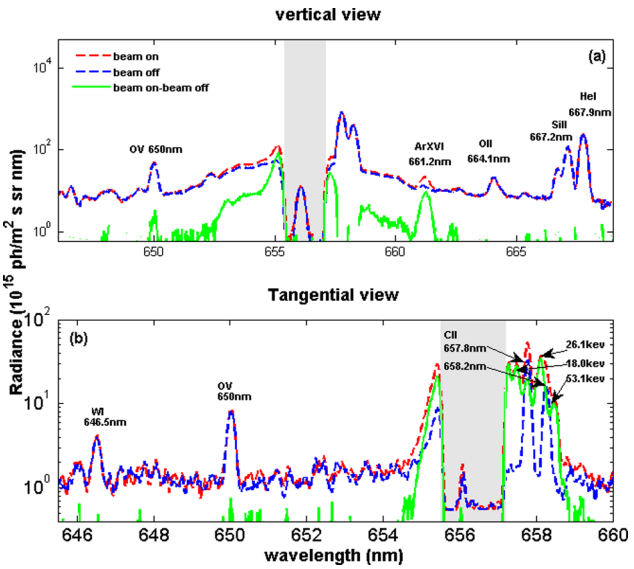

FIG. 6. Raw data of FIDA at discharge #61821. Spectra collected by (a) Bunkoukeiki from vertical view and (b) by Kaiser from tangential view.

present in the blue-shifted wing of the cold D_α line. Thus for the coming application of f-FIDA using photomultipliers, a band-pass filter with a pass-band of 3 nm centered at 653.0 nm will be applied. As the shapes of impurity lines (OV, OII, etc.) in active spectral (red lines) are in excellent agreement with passive ones (blue lines), beam modulation method is reliable. The core ion temperature is about 1.1 keV obtained by X-ray crystal spectrometer;[13] thus, the halo's thermal broadening is about 1.2 nm. The roughly calculated halo matches the net signal (green lines) well; the FIDA signal and halo can be separated with the employment of FIDASIM.

Fig. 6(b) shows the spectrum from tangential view at R = 201 cm measured by Kaiser system. With different geometry, beam emission lines and co-current fast-ion feature appeared in the red-shifted wing, overlapped with two CII lines. According to the Doppler shift 2.46 nm, 1.72 nm, and 1.43 nm, the calculated beam energy is as 53.1 keV, 26.1 keV, and 18.0 keV, which is exactly corresponding to the full, half, and third energetic beam neutrals. The study of the radial distribution of fast ion density is on-going. The tangential views are designed to study fast-ion feature with a counter-current injection on F-port (see Fig. 1). Once the counter-neutral sources are employed, fast ion feature will be blue-shifted and red-shifted while the beam emission is red-shifted. Therefore, fast-ion feature in blue wing will be available.

ACKNOWLEDGMENTS

We would like to express our gratitude to K. Ida for the helpful discussion. This work was supported by the National Natural Science Foundation of China Grant No. 11575249 and National Magnetic Confinement Fusion Energy Research Program under Grant Nos. 2015GB110005, 2014GB109004, 2012GB101001, and 2015GB120002.

[1]W. W. Heidbrink, Rev. Sci. Instrum. **81**, 10D727 (2010).
[2]W. W. Heidbrink, K. H. Burrell, Y. Luo, N. A. Pablant, and E. Ruskov, Plasma Phys. Controlled Fusion **46**, 1855 (2004).
[3]M. Podestà, W. W. Heidbrink, R. Bell, and R. Feder, Rev. Sci. Instrum. **79**, 10E521 (2008).
[4]E. Delabie, R. J. Jaspers, M. G. Von Hellermann, S. K. Nielsen, and O. Marchuk, Rev. Sci. Instrum. **79**, 10E522 (2008).
[5]M. Osakabe, S. Murakami, M. Yoshinuma, K. Ida, A. Whiteford, M. Goto, D. Kato, T. Kato, K. Nagaoka, T. Tokuzawa, Y. Takeiri, and O. Kaneko, Rev. Sci. Instrum. **79**, 10E519 (2008).
[6]B. Geiger, M. Garcia-Munoz, W. W. Heidbrink, R. M. McDermott, G. Tardini, R. Dux, R. Fischer, V. Igochine, and ASDEX Upgrade Team, Plasma Phys. Controlled Fusion **53**, 065010 (2011).
[7]C. Michael, N. Conway, B. Crowley, O. Jones, W. W. Heidbrink, S. Pinches, E. Braeken, R. Akers, C. Challis, M. Turnyanskiy, A. Patel, D. Muir, R. Gaffka, and S. Bailey, Plasma Phys. Controlled Fusion **55**, 095007 (2013).
[8]J. Huang, W. W. Heidbrink, B. Wan, M. G. von Hellermann, Y. Zhu, W. Gao, C. Wu, Y. Li, J. Fu, B. Lyu, Y. Yu, Y. Shi, M. Ye, L. Hu, and C. Hu, Rev. Sci. Instrum. **85**, 11E407 (2014).
[9]Y. B. Zhu, J. Z. Zhang, M. Z. Qi, S. B. Xia, D. Liu, W. W. Heidbrink, B. N. Wan, and J. G. Li, Rev. Sci. Instrum. **85**, 11E107 (2014).
[10]Y. Zhang, Y. Li, J. Fu, X. Yin, B. Lyu, Y. Shi, X. Du, Q. Wang, Y. Yu, M. Ye, and B. Wan, Fusion Eng. Des. **96–97**, 840–843 (2015).
[11]J. Huang *et al.*, Rev. Sci. Instrum. **87**, 11E542 (2016).
[12]B. Geiger, R. Dux, R. M. McDermott, S. Potzel, M. Reich, F. Ryter, M. Weiland, D. Wünderlich, ASDEX Upgrade Team, and M. Garcia-Munoz, Rev. Sci. Instrum. **84**, 113502 (2013).
[13]B. Lyu, F. D. Wang, X. Y. Pan, J. Chen, J. Fu, Y. Y. Li, M. Bitter, K. W. Hill, L. F. Delgado-Aparicio, N. Pablant, S. G. Lee, Y. J. Shi, M. Y. Ye, and B. N. Wan, Rev. Sci. Instrum. **85**, 11E406 (2014).